DOI 10.1007/s00249-016-1157-7

Molecular basis and quantitative assessment of TRF1 and TRF2 protein interactions with TIN2 and Apollo peptides

Umesh Kalathiya[1] · Monikaben Padariya[1] · Maciej Baginski[1]

Abstract Shelterin is a six-protein complex (TRF1, TRF2, POT1, RAP1, TIN2, and TPP1) that also functions in smaller subsets in regulation and protection of human telomeres. Two closely related proteins, TRF1 and TRF2, make high-affinity contact directly with double-stranded telomeric DNA and serve as a molecular platform. Protein TIN2 binds to TRF1 and TRF2 dimer-forming domains, whereas Apollo makes interaction only with TRF2. To elucidate the molecular basis of these interactions, we employed molecular dynamics (MD) simulations of $TRF1_{TRFH}$-$TIN2_{TBM}$ and $TRF2_{TRFH}$-$TIN2_{TBM}$/$Apollo_{TBM}$ complexes and of the isolated proteins. MD enabled a structural and dynamical comparison of protein–peptide complexes including H-bond interactions and interfacial residues that may regulate TRF protein binding to the given peptides, especially focusing on interactions described in crystallographic data. Residues with a selective function in both $TRF1_{TRFH}$ and $TRF2_{TRFH}$ and forming a stable hydrogen bond network with $TIN2_{TBM}$ or $Apollo_{TBM}$ peptides were traced. Our study revealed that $TIN2_{TBM}$ forms a well-defined binding mode with $TRF1_{TRFH}$ as compared to $TRF2_{TRFH}$, and that the binding pocket of $TIN2_{TBM}$ is deeper for $TRF2_{TRFH}$ protein than $Apollo_{TBM}$. The MD data provide a basis for the reinterpretation of mutational data obtained in crystallographic work for the TRF proteins. Together, the previously determined X-ray structure and our MD provide a detailed view of the TRF–peptide binding mode and the structure of TRF1/2 binding pockets. Particular TRF–peptide interactions are very specific for the formation of each protein–peptide complex, identifying TRF proteins as potential targets for the design of inhibitors/drugs modulating telomere machinery for anticancer therapy.

Keywords Shelterin complex · Molecular dynamics · TRF1 · TRF2 · TIN2 · Apollo

Introduction

Telomeres are nucleoprotein complexes and specialized heterochromatic structures present at the ends of eukaryotic chromosomes that ensure their proper function. A group of proteins interacting with telomeric DNA is named the shelterin complex, which includes TRF1 and TRF2, which in turn recruit RAP1, TIN2, TPP1, and POT1 (deLange 2005; Broccoli et al. 1997). In particular, TRF1 (Telomere Repeat Binding Factor 1) interacts specifically with the duplex DNA and is implicated in telomere replication, telomere protection, and telomere length maintenance (deLange 2005; Broccoli et al. 1997; Smogorzewska et al. 2000; Weisi et al. 2013). TRF2 (Telomere Repeat Binding Factor 2) was identified as a TRF1 paralog and TIN2 (TRF1 Interacting Nuclear Factor 2) and Rap1 were found via two-hybrid screen to interact with TRF1 and TRF2, respectively (deLange 2005; Broccoli et al. 1997; Smogorzewska et al. 2000; Weisi et al. 2013; Jason et al. 2012). TPP1 (also termed TINT1, PTOP, or PIP1) was identified as a TIN2-interacting protein (deLange 2005; Xin et al. 2007; Liu et al. 2004; Kim et al. 1999; Ye et al. 2004a).

[1] Department of Pharmaceutical Technology and Biochemistry, Faculty of Chemistry, Gdansk University of Technology, Narutowicza St 11/12, 80-233 Gdansk, Poland

POT1 (Protection of Telomere 1) was discovered based on sequence homology to telomere end-binding factors in unicellular eukaryotes (Lei et al. 2004; Baumann and Cech 2001).

Shelterin proteins have specific properties that make them different from other DNA-binding proteins on several criteria (deLange 2005; Jason et al. 2012; Kim et al. 1999). They are found abundantly at chromosome ends and are present at telomeres throughout the cell cycle, and their known functions are limited to telomeres. All these six proteins form a DNA protecting complex that allows cells to differentiate the end of telomeric DNA from sites of DNA damage (deLange 2005; Liu et al. 2004; Lei et al. 2004; Baumann and Cech 2001; Chen et al. 2008; Walker and Zhu 2012; vanSteensel et al. 1998). All shelterin subunits can be found in a single complex in fractionated nuclear extracts. TRF1, TRF2, and POT1 proteins directly recognize TTAGGG repeats present in telomeric DNA. TPP1 interacts with TIN2 as well as with POT1, and Rap1 interacts with TRF2 (deLange 2005; Weisi et al. 2013; Jason et al. 2012; Kim et al. 1999). The cohesive source of support and stability of the complex is TIN2 protein, which connects to TRF1, TRF2, and TPP1/POT1 heterodimer (Weisi et al. 2013; Walker and Zhu 2012; vanSteensel et al. 1998; Frescas and deLange 2014). TIN2 was found to bind TRF1 and TRF2 simultaneously, and this link contributes to the stabilization of TRF2 on telomeres. TIN2-mediated co-operative binding of TRF1 and TRF2 to telomeres has an important role for the mechanism of telomere length regulation and protection (Liu et al. 2004; Walker and Zhu 2012; Bianchi et al. 1997; Ye et al. 2004b).

In spite of having low sequence similarity (27 % sequence identity) (Fairall et al. 2001; Hanaoka et al. 2005), TRF1 and TRF2 are homologous proteins that share common 3D structural formations consisting of an N-terminal domain, a TRF homology domain (TRFH), which mediates dimerization, a flexible linker region (FLR), and a C-terminal SANT/Myb-like DNA binding domain (Walker and Zhu 2012; Bianchi et al. 1997, 1999; Fairall et al. 2001; Court et al. 2005). TRF1 and TRF2 both have a DNA binding domain and dimer-forming domain, and individually they form homodimers and higher-order oligomers (Fairall et al. 2001). Since TRFH domains are connected through protein–protein interactions (TIN2 is involved in this interaction), these proteins of the shelterin complex have the capacity to recognize telomeric DNA with at least five DNA-binding domains, two each in TRF1 and TRF2 and one in POT1 (deLange 2005; Court et al. 2005; Bianchi et al. 1999). TRF1 recognizes TIN2 using a conserved molecular surface in its TRFH domain. However, this same surface does not act as a TIN2 binding site for TRF2 and binding of TIN2 to TRF2 is mediated by a region outside the TRFH domain (Chen et al. 2008). Alternatively, the TRFH docking site of TRF2 binds a shelterin accessory factor (Apollo), which does not interact with the TRFH domain of TRF1 (Chen et al. 2008). The binding of Apollo to the TRFH domain of TRF2 is required for the telomeric localization of Apollo, and Apollo functions together with TRF2 in protecting telomeres (Chen et al. 2008).

The shelterin complex functions not only to protect telomeres from being recognized as double strand breaks but also to maintain telomere length homeostasis that is associated with tumorigenesis and aging (deLange 2005; Okamoto et al. 2008). Telomere dysfunction is believed to be a significant factor in carcinogenesis. Reduced expression of TRF1 is associated with tumor progression and poor prognosis in carcinoma (Hu et al. 2010; Chuang et al. 2011). Due to the fact that TRF proteins bind to DNA, they play a key biological role at the ends of telomeres. The nucleoprotein complex of TRF with DNA creates a docking platform for other shelterin proteins and the TRFH domain of both proteins is responsible for this property (DiMaro et al. 2014). Interaction between TRFH and TIN2 is the central point of the shelterin complex. Therefore, it is crucial to understand how the two members of this binary system (TRF-TIN2) interact at a molecular level (DiMaro et al. 2014). Since this is expected to be a very selective interaction, one may assume that it can be used as a potential target for the design of compounds modulating telomere machinery and also for designing inhibitors/drugs for anticancer therapy. Some supporting data confirming this type of approach have been recently published (DiMaro et al. 2014). Using TRF proteins as potential targets in chemotherapy can be especially valuable because telomeres in cancer cells are usually shorter and more fragile than in regular cells (Diehl et al. 2011). Therefore any intervention in telomere machinery may be more damaging for cancer cells than regular ones (Kim et al. 2009; Bidzinska et al. 2014).

It has been shown that molecular dynamics (MD) simulation is a tool complementary to experimental approaches (vanGunsteren and Mark 1992). Experimental information can be used in a computer simulation to limit the potentially enormous range of configurational space accessible to a biomolecular system, to a region of specific interest (active site). On the other hand, a computer simulation can augment and help the understanding of experimental information by providing a detailed picture of structure, energetics, and dynamics at an atomic level (vanGunsteren and Mark 1992). Almost all available studies on TRF1 and TRF2 protein have focused on experimental methods to study peptide recognition towards these proteins and provided only static details about the interactions of peptides (TIN2 and Apollo) to TRF1 and TRF2 (Chen et al. 2008). Thus, dynamic details of protein–peptide interactions at a molecular level are lacking. Hence, in this study, we have carried out molecular dynamics simulations for 1000 ns on

$TRF1_{TRFH}$ (TRFH = TRF homology domain) protein in complex with $TIN2_{TBM}$ (TBM = TRF-binding motif) and $TRF2_{TRFH}$ protein in complex with $TIN2_{TBM}$/$Apollo_{TBM}$. Molecular dynamics results advance our knowledge of the structural and molecular properties of peptide recognition in $TRF1_{TRFH}$ and $TRF2_{TRFH}$ proteins. The MD results were compared with experimental data (Chen et al. 2008) to provide some new observations on the dynamic behavior of TRF_{TRFH} proteins. The molecular details of protein–peptide recognition we obtained extend our knowledge about these complexes and provide a basis for exploring inhibitor design.

Materials and methods

Starting structures

Protein structures (obtained from X-ray studies) for TRFH (TRFH = TRF homology domain) domains of $TRF1_{TRFH}$ and $TRF2_{TRFH}$ proteins were retrieved from the protein data bank (PDB). Structures of the TRF homology domain of TRF1 and TRF2 protein are available in complex with $TIN2_{TBM}$ or $Apollo_{TBM}$ peptide (for TIN2 and Apollo protein, only part of its whole protein structure is available, hence, here it is referred to as a peptide). TRF homology domain structures used for this study are: (1) the structure of $TRF1_{TRFH}$ containing $TIN2_{TBM}$ peptide (PDB ID: 3BQO) (Chen et al. 2008), (2) $TRF2_{TRFH}$ containing $TIN2_{TBM}$ peptide (PDB ID: 3BU8) (Chen et al. 2008), and (3) $TRF2_{TRFH}$ with $Apollo_{TBM}$ peptide (PDB ID: 3BUA) (Chen et al. 2008) (Fig. S1). Missing N and C terminal residues in the structures of $TRF1_{TRFH}$ and $TRF2_{TRFH}$ proteins were not considered as they are not located near interacting (binding) regions of the respective peptide. Moreover, the PDB structure of the $TIN2_{TBM}$ peptide slightly differs when it is in complex with $TRF1_{TRFH}$ and $TRF2_{TRFH}$ protein. In our study, we have used protein–peptide coordinates as available in the original PDB file in order to maintain same positions obtained from experimental (X-ray) studies (Chen et al. 2008). Apart from protein–peptide complexes, structures alone (without respective partners) for $TRF1_{TRFH}$, $TRF2_{TRFH}$, $TIN2_{TBM}$, and $Apollo_{TBM}$ were also considered for molecular dynamics calculations to understand behavior of protein or peptide when they are alone in an environment with solvent and ions.

Molecular dynamics simulations

The all-atom structure of $TRF1_{TRFH}$ and $TRF2_{TRFH}$ protein in complex with $TIN2_{TBM}$ or $Apollo_{TBM}$ peptide, and structures of protein and peptide alone were prepared and their structure minimized using Discovery Studio Client 3.1 software [BIOVIA—former Accelrys, San Diego, CA, USA]. Seven different systems were prepared on which molecular dynamics calculations were performed using GROMACS (GROningen MAchine for Chemical Simulations) version 4.6 (Hess et al. 2008): (1) $TRF1_{TRFH}$ with $TIN2_{TBM}$ (Fig. S1), (2) $TRF2_{TRFH}$ with $TIN2_{TBM}$ (Fig. S1), (3) $TRF2_{TRFH}$ with $Apollo_{TBM}$ (Fig. S1), (4) $TRF1_{TRFH}$ (alone), (5) $TRF2_{TRFH}$ (alone), (6) $TIN2_{TBM}$ (alone), and (7) $Apollo_{TBM}$ (alone).

Numerical procedures in molecular mechanics (MM) and dynamics (MD) simulation were as follows: (a) Protein/peptide system set up: For all prepared systems, water molecules present in the original protein/peptide structure were removed and the protein or peptide or complex (protein–peptide) was kept in a TIP3P box of water molecules with ~0.15 M NaCl, to neutralize the protein/peptide. A rhombic dodecahedron box with 1 nm edge was used as it provides a more effective packing of periodic images than rectangular boxes. (b) Protein/peptide structure optimization: During the optimization step, hydrogen atoms absent in the original protein structures were added and systems were optimized until the local minimum of the system was found using the steepest-descent method (Arfken 1985). All chemical bonds between the atoms of the protein/peptide were constrained using LINear Constraint Solver denoted by the LINCS algorithm (Hess et al. 1997) in GROMACS. Each molecular system was energy minimized until the minimal energy was obtained using a steepest-descent algorithm with a total number of steps of 2000. Convergence of the system was achieved by minimizing the solvent energy above 10 kcal/mol, after which an equilibration phase was implemented to gradually heat the system from 0.1 to 300 K by applying isothermal-isobaric conditions (NPT). (c) MD simulation: Molecular dynamics simulations were then performed over a period of 1000 ns using the GROMACS simulation software package with the CHARMM27 forcefield (Bjelkmar et al. 2010). Simulations were run at 300 K with a coupling constant of 0.1 ps and constant temperature was maintained by the V-rescale algorithm (Bussi et al. 2007). Periodic boundary conditions (Makov and Payne 1995) were applied in conjunction with the particle mesh Ewald method to account for electrostatic forces in the system (Darden et al. 1993). Coordinates obtained from molecular dynamics calculations were saved every 10 ps and were used for analysis of TRF protein structural and molecular properties in the presence and absence of the respective peptides.

Results and discussion

Molecular dynamics (MD) results provided detailed analysis on structural properties and dynamic effects of

$TRF1_{TRFH}$ and $TRF2_{TRFH}$ proteins in the presence and absence of bound peptides. It has been observed from molecular dynamics calculations that in spite of having structural similarities, both proteins $TRF1_{TRFH}$ and $TRF2_{TRFH}$ behave differently in the presence and absence of peptide. Peptides have a high degree of freedom, and different conformational changes in their structure in the presence or absence of respective TRFH domains of TRF proteins were observed (Fig. 1, S2, S3, and S4). During 1000 ns of MD simulation time, there were also various similarities and differences observed in the structures of the $TRF1_{TRFH}$ and $TRF2_{TRFH}$ domains of the TRF1 and TRF2 proteins, respectively.

Stability of TRF protein systems

Obtained trajectories from molecular dynamics simulations were judged to be stable, as evidenced by the time-dependent evaluation of RMSD (root-mean-square deviations). Equilibration and stability of each system was checked by calculating the RMSD values of protein or peptide separately and in protein–peptide complexes. Figure 2 shows RMSD values obtained from the MD trajectory of each studied system. Molecular dynamics simulations of $TRF1_{TRFH}$ and $TRF2_{TRFH}$ protein were performed in the presence and absence of peptide; the isolated peptides were also simulated for 1000 ns. Obtained results suggest that when the proteins ($TRF1_{TRFH}$ or $TRF2_{TRFH}$) lack peptide, they have higher RMSD values, and the same was observed for the isolated peptides (Fig. 2).

However, whereas in the absence of the $TIN2_{TBM}$ peptide, RMSD values for $TRF1_{TRFH}$ protein reached up to ~10 Å, for the $TRF2_{TRFH}$ protein there was only a slight increase in RMSD without peptide bound. The rise in RMSD values for $TRF1_{TRFH}$ was linked to conformational changes in the N and C terminal residues (specifically C terminal residues from 261-268) of the protein (Figs. 2, 3a), far from the peptide binding site. On the other hand, during MD simulation, it was observed that the overall RMSD values of $TRF2_{TRFH}$ protein in peptide bound and unbound form are less than those for the $TRF1_{TRFH}$ protein (Fig. 2) and are not changing noticeably after $TIN2_{TBM}$ binding (for $TRF2_{TRFH}$ protein). The binding of $TRF1_{TRFH}$ by $TIN2_{TBM}$ peptide lowers the RMSD of the protein comparatively more than binding of the same peptide to $TRF2_{TRFH}$ protein. Thus, RMSD and RMSF analysis of peptide bound and unbound forms

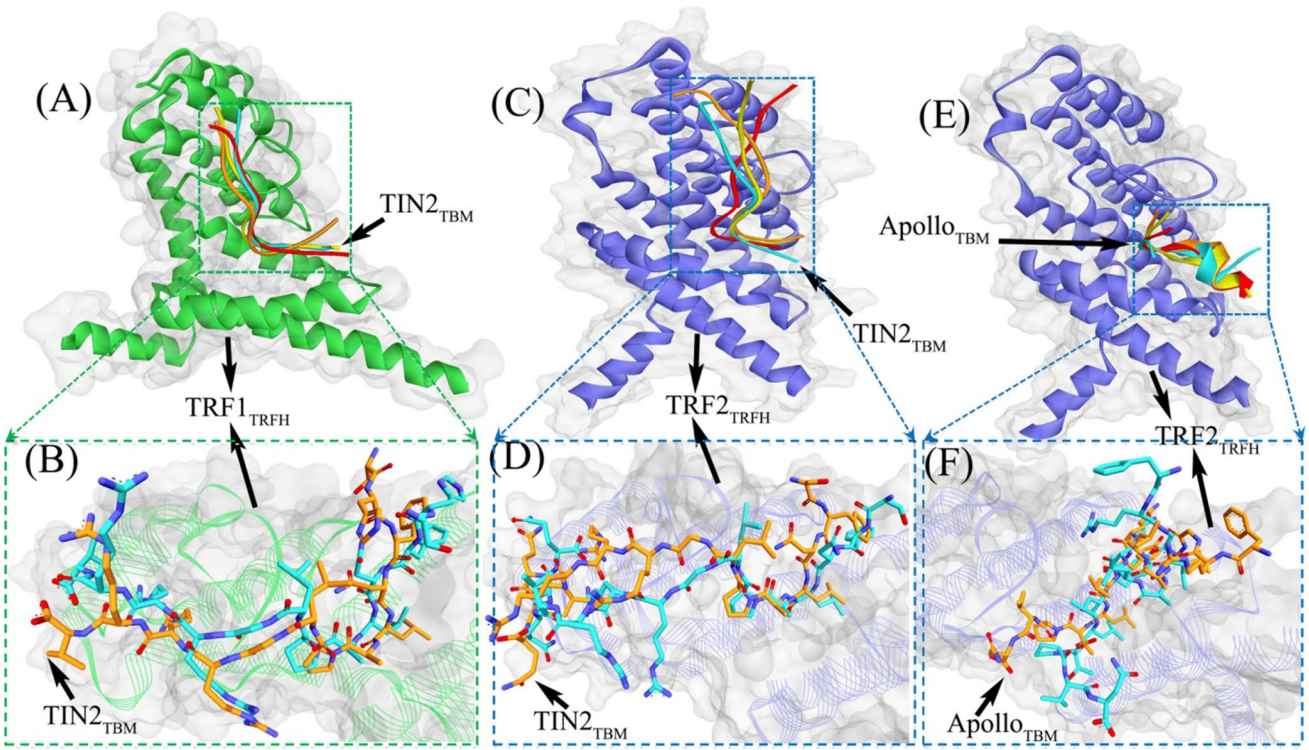

Fig. 1 $TRF1_{TRFH}$ and $TRF2_{TRFH}$ protein in complex with $TIN2_{TBM}$ or $Apollo_{TBM}$ peptide, respectively. **a**, **c**, **e** Conformational change of the peptide at the beginning, middle, and end of each simulation. Protein is represented as a *ribbon/surface* and peptide is represented as *solid ribbon*. (*Color* $TRF1_{TRFH}$ in *green*, $TRF2_{TRFH}$ in *blue*, peptide in *orange* is from beginning, peptide in *yellow* and *red* is at the middle of simulation time, and peptide in *blue* is at the end of simulation time). For **b**, **d**, **f**, carbon atoms colored *orange* represent peptide at the beginning, and *blue* shows peptide at the end of the MD simulation

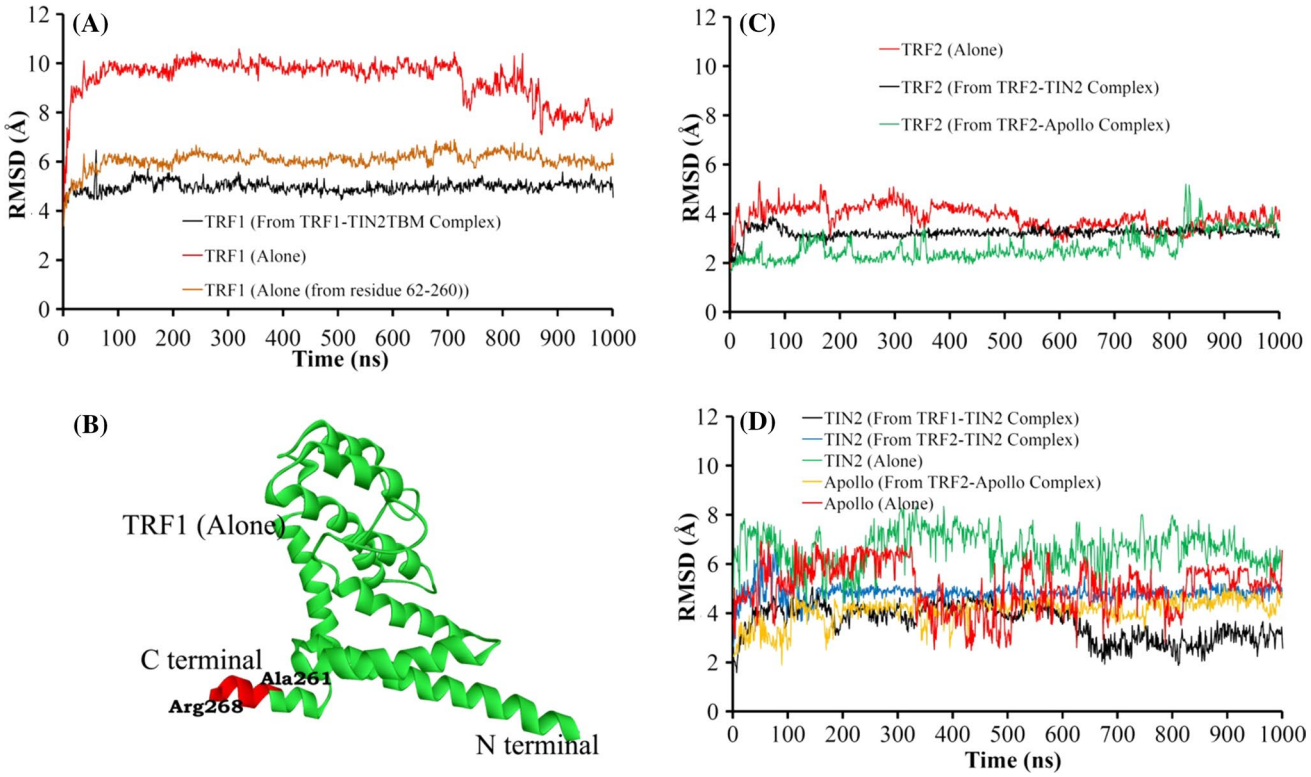

Fig. 2 RMSD of $TRF1_{TRFH}$, $TRF2_{TRFH}$, $TIN2_{TBM}$, and $Apollo_{TBM}$. **a** RMSD plot of $TRF1_{TRFH}$ protein in complex with $TIN2_{TBM}$ peptide, $TRF1_{TRFH}$ alone (without $TIN2_{TBM}$), and $TRF1_{TRFH}$ alone excluding C terminal residues 261–268. **b** Isolated $TRF1_{TRFH}$ structure showing N and C terminal residues excluded for calculating RMSD. **c** RMSD plot of $TRF2_{TRFH}$ protein in complex with $TIN2_{TBM}$/$Apollo_{TBM}$ peptide and alone. **d** RMSD of $TIN2_{TBM}$ and $Apollo_{TBM}$ peptides in the absence of their respective partners, and from $TRF1_{TRFH}$-$TIN2_{TBM}$, $TRF2_{TRFH}$-$TIN2_{TBM}$, and $TRF2_{TRFH}$-$Apollo_{TBM}$ complexes

of the $TRF1_{TRFH}$/$TRF2_{TRFH}$ protein (Figs. 2, 3) show that $TRF1_{TRFH}$ comparatively gets more ordered (by induced fit) in its structure near the peptide binding region than $TRF2_{TRFH}$. At the same time, with respect to the $TIN2_{TBM}$ peptide, more conformational change over the simulation time course was observed when it was bound to $TRF2_{TRFH}$ than to $TRF1_{TRFH}$ (Fig. 1). The RMSD plot of the $TIN2_{TBM}$ peptide shows that it has higher RMSD values (Fig. 2d) when bound with the $TRF2_{TRFH}$ protein than bound to the $TRF1_{TRFH}$ protein (Fig. 3), indicating that the $TIN2_{TBM}$ peptide-$TRF1_{TRFH}$ protein complex is more stable than the $TRF2_{TRFH}$ complex. On this point, one should remember that the $TRF2_{TRFH}$ protein interacts with both $TIN2_{TBM}$ peptide and other shelterin accessory factors (e.g., $Apollo_{TBM}$) (Chen et al. 2008), and such flexibility as it is observed for $TIN2_{TBM}$ in its RMSD values (Fig. 2d) while interacting with $TRF2_{TRFH}$ may allow for the recognition of other peptides, whereas $TRF1_{TRFH}$ protein interacts only with $TIN2_{TBM}$ (Chen et al. 2008). To conclude the RMSD analysis, we argue that since $TRF1_{TRFH}$ recognizes only one peptide ($TIN2_{TBM}$) (Chen et al. 2008) binding of this peptide to $TRF1_{TRFH}$ is very selective and associated with protein induce fit, whereas $TRF2_{TRFH}$ protein is able to recognize different peptides (Chen et al. 2008) and therefore binding of these peptides ($TIN2_{TBM}$ or $Apollo_{TBM}$) does not comparatively involve an induced fit with the $TRF2_{TRFH}$ protein.

Although the detailed behavior of $TRF1_{TRFH}$ and $TRF2_{TRFH}$ bound to $TIN2_{TBM}$ or $Apollo_{TBM}$ peptides varied for each specific pairing, in each case the binding of a peptide stabilizes the $TRF1_{TRFH}$ or $TRF2_{TRFH}$ structure, and also results in stabilization of the peptide ($TIN2_{TBM}$ or $Apollo_{TBM}$). These observations suggest that the peptides play an important role in the stabilization of the $TRF1_{TRFH}$ or $TRF2_{TRFH}$ domains of the TRF proteins, and that the peptides are stabilized in each case by becoming protein bound (Fig. 2). The RMSD values for all three protein–peptide complexes were not higher than ~5 Å and remained almost steady over the simulation time (Fig. 2).

Conformational changes and flexibility

In order to evaluate and compare conformational fluctuations of $TRF1_{TRFH}$ and $TRF2_{TRFH}$ proteins alone and in complex with $TIN2_{TBM}$ or $Apollo_{TBM}$ peptides, root mean square fluctuations (RMSFs) of each amino acid residue

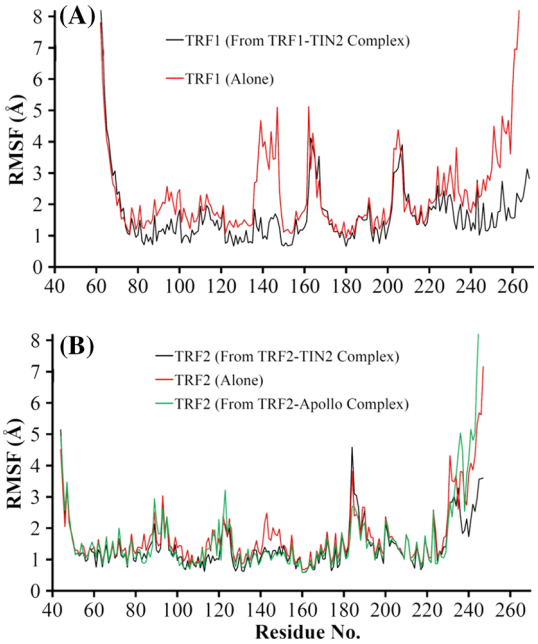

Fig. 3 Root mean-square fluctuation (RMSF) as a function of residue number computed for C^{α} atoms of all six model systems of TRF proteins. **a** RMSF of $TRF1_{TRFH}$ protein in the simulation of $TRF1_{TRFH}$ alone and in the $TRF1_{TRFH}$-$TIN2_{TBM}$ complex (peptide interacting residues: 104–112 and 125–155). **b** RMSF values of $TRF2_{TRFH}$ protein alone and in complex of $TRF2_{TRFH}$-$TIN2_{TBM}$/$Apollo_{TBM}$ (peptide interacting residues for $TRF2_{TRFH}$-$TIN2_{TBM}$/$Apollo_{TBM}$ complex are from: 82–129)

were generated (Fig. 3). Different conformations of the respective peptides with TRF proteins (Fig. 1, S2, S3, and S4) were also analyzed. As shown in Fig. 3, the RMSF calculation indicates that residues in $TRF1_{TRFH}$ protein fluctuate within the range of ~0.6–15 Å (~15 Å RMSF was observed for C terminal residues), and the fluctuation ranges for $TRF1_{TRFH}$ protein were similar without and with peptide bound. High differences in the RMSF fluctuation for peptide bound and unbound systems of $TRF1_{TRFH}$ protein were observed only in the region where the peptide binds to protein (Fig. 3a), and this observation supports the idea of protein induce fit after peptide binding. $TRF2_{TRFH}$ protein in $TIN2_{TBM}$ peptide bound and unbound systems had a fluctuation range of ~ 0.6–7.0 Å (maximum fluctuation were observed in C terminal residues) (Fig. 3b). The same level of average fluctuation except at the N and C terminal residues of the $TRF2_{TRFH}$ protein in the $TRF2_{TRFH}$-$Apollo_{TBM}$ complex were also observed (Fig. 3b). Similar to $TRF1_{TRFH}$ protein, for $TRF2_{TRFH}$ protein also a slight difference in RMSF fluctuation for peptide bound and unbound systems were observed in the region where the peptide ($TIN2_{TBM}$ or $Apollo_{TBM}$) binds to the protein (Fig. 3). This observation is consistent with the idea that both peptides ($TIN2_{TBM}$ or $Apollo_{TBM}$) bind to a rather rigid $TRF2_{TRFH}$ with comparatively less induced fit compared to the $TRF1_{TRFH}$-$TIN2_{TBM}$ complex.

A significant difference in RMSF fluctuation for protein alone (peptide unbound) and protein–peptide (peptide bound) systems were observed, which indicated that the presence of peptide ($TIN2_{TBM}$ or $Apollo_{TBM}$) is responsible for fluctuation and conformational changes in residues of TRF proteins. This phenomenon is particularly observed in the case of the $TRF1_{TRFH}$ protein (Fig. 3a). In general, we observed that peptides ($TIN2_{TBM}$ or $Apollo_{TBM}$) try different ways to fit onto target proteins ($TRF1_{TRFH}$ or $TRF2_{TRFH}$), adopting a range of conformations in the process (Fig. 1, S2, S3, and S4). Because $TIN2_{TBM}$ or $Apollo_{TBM}$ peptide suppressed the fluctuating residues of TRF proteins in protein–peptide complexes, we made a more detailed analysis of protein–peptide and protein–water interactions in each case. We selected a range of residues to analyze for this on the basis that their RMSF is lowered in the respective protein–peptide complex compared to the peptide-unbound systems: for $TRF1_{TRFH}$ residues 104-112 and 125-155, and for $TRF2_{TRFH}$ residues 80-129 and 130-135.

Generally, in structural regions of protein, its nine α-helices are better defined and tend to be less flexible than its other regions. During MD calculations of all complexes, RMSF data indicated more fluctuations of segments belonging to loops (except loops where peptide binds) that connect secondary structure elements e.g., residues range 134-150 in $TRF1_{TRFH}$-$TIN2_{TBM}$ complex, residues range 143–149 and 183–189 in $TRF2_{TRFH}$-$TIN2_{TBM}$ complex and residues range 88–95 and 115–127 of $TRF2_{TRFH}$-$Apollo_{TBM}$ complex. While these features are common to all complexes, $TRF2_{TRFH}$ protein shows a different mobility when it binds to $TIN2_{TBM}$ (residues range 82–129 in $TRF2_{TRFH}$-$TIN2_{TBM}$) or $Apollo_{TBM}$ peptides (residues range 80–129 in $TRF2_{TRFH}$-$Apollo_{TBM}$), as the certain values of the RMSF differ and cause reduction in fluctuations (conformational changes) in the next loop near to the binding site (residues range 142–149 in $TRF2_{TRFH}$-$TIN2_{TBM}$ and residues range 143–151 in $TRF2_{TRFH}$-$Apollo_{TBM}$ complex).

Hot spot residues of TRF_{TRFH} proteins involved in binding with $TIN2_{TBM}$ or $Apollo_{TBM}$

Protein–peptide interactions play important roles in many cellular processes. Protein conformational changes upon binding, an ill-defined peptide binding surface and the large number of peptide degrees of freedom make the prediction of protein–peptide interactions particularly challenging but on the other hand these interactions are very selective (Dagliyan et al. 2011). Hydrogen bonds are the most important specific interactions in biological recognition processes and they are one of the major driving forces to

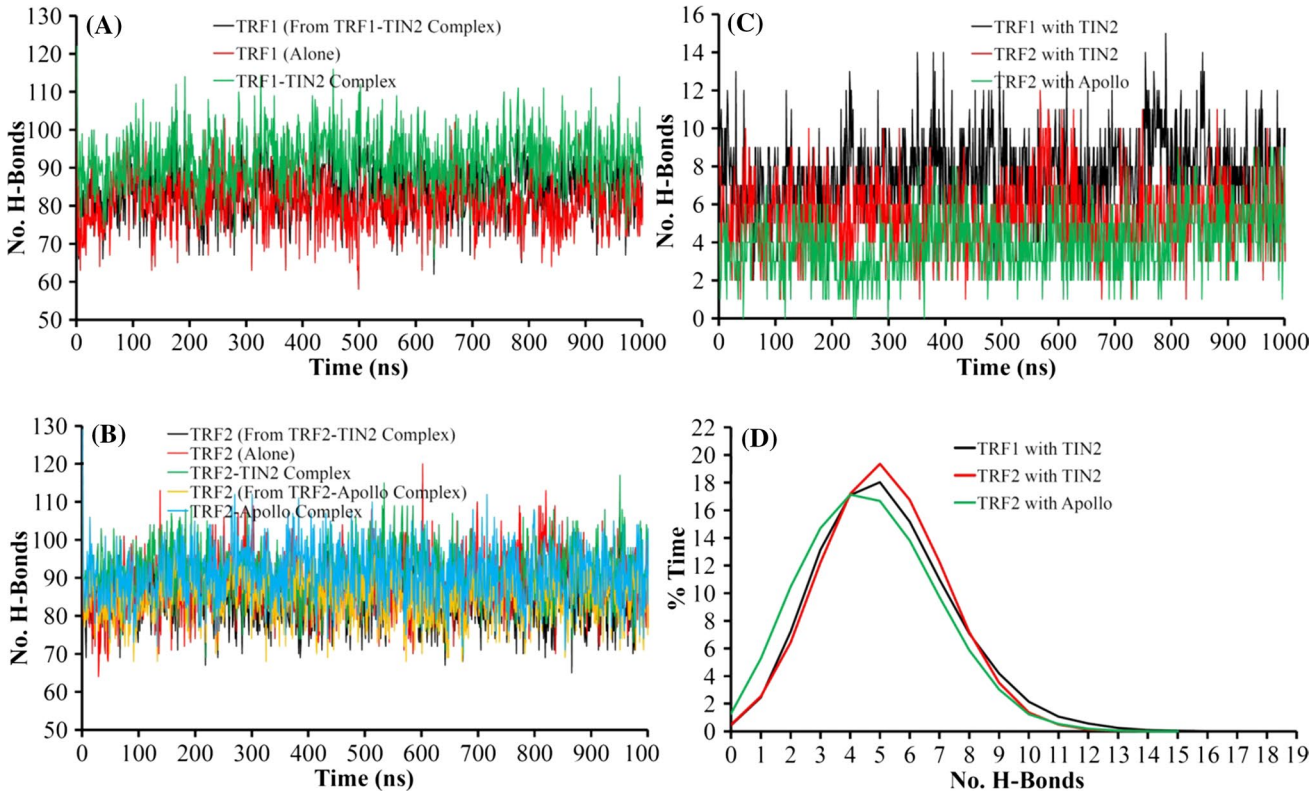

Fig. 4 Intramolecular and intermolecular interactions of $TRF1_{TRFH}$-$TIN2_{TBM}$, $TRF2_{TRFH}$-$TIN2_{TBM}$, and $TRF2_{TRFH}$-$Apollo_{TBM}$ complexes. **a**, **b** Intramolecular interactions of TRF protein with and without peptide, and for the whole complex. **c** Intermolecular interaction of TRF protein with their respective peptides. **d** Hydrogen bond distribution of $TRF1_{TRFH}$ with peptide $TIN2_{TBM}$ and $TRF2_{TRFH}$ with peptide $TIN2_{TBM}$ or $Apollo_{TBM}$, respectively. The peaks of the graph represent stability and number of hydrogen bonds formed during simulation

stabilize, e.g., α-helix, β-sheet, and other secondary structures. Thus, the effects arising from the making and breaking of hydrogen bonds are responsible for much of the biological activity of proteins (Dagliyan et al. 2011; Sheu et al. 2003). Figure 4 represents intramolecular interactions for protein in complex or alone and for the protein–peptide complex. Intermolecular interactions of TRF protein with the respective peptides of all three complexes ($TRF1_{TRFH}$-$TIN2_{TBM}$, $TRF2_{TRFH}$-$TIN2_{TBM}$, and $TRF2_{TRFH}$-$Apollo_{TBM}$) are also shown in Fig. 4. Analyzing intramolecular interactions within each TRF protein when alone and within a protein–peptide complex (Fig. 4a, b) shows that all three protein–peptide complex have almost the same number of H-bonds. On the other hand, the intermolecular interactions of TRF proteins with their respective partners (Fig. 4c) show the $TRF1_{TRFH}$-$TIN2_{TBM}$ complex has formed more H-bonds than the other two systems and that the TRFH domain of the TRF2 protein has more interactions with $TIN2_{TBM}$ compared to with $Apollo_{TBM}$. This shows why the $TIN2_{TBM}$ peptide has formed a well-defined binding mode with $TRF1_{TRFH}$ as compared to $TRF2_{TRFH}$ and these results correlate with RMSD plots of $TIN2_{TBM}$ (Fig. 2): $TIN2_{TBM}$ is more stable with less RMSD fluctuations and degrees of freedom in the $TRF1_{TRFH}$-$TIN2_{TBM}$ complex than the $TRF2_{TRFH}$-$TIN2_{TBM}$ complex (Figs. 1, 2).

To analyze in detail how many intermolecular H-bonds are formed during 1000 ns of simulation time, the frequency of H-bonds was calculated for all three protein–peptide complexes (Fig. 4d). Frequency values (Fig. 4d) correlate well with intermolecular interaction plots over the time course (Fig. 4c) and show that the $TRF1_{TRFH}$-$TIN2_{TBM}$ complex has formed more H-bonds compared to the other studied systems (Fig. 4d), and that the TRFH domain of TRF2 protein has more interactions with $TIN2_{TBM}$ as compared to $Apollo_{TBM}$ peptide. The $TRF1_{TRFH}$ and $TRF2_{TRFH}$ proteins with $TIN2_{TBM}$ peptide show a maximum of five hydrogen bonds lasting ~19 % of the total simulation time whereas, $TRF2_{TRFH}$ forms a maximum of four hydrogen bonds with $Apollo_{TBM}$ peptide lasting 17 % of the total simulation time (Fig. 4d). Analyzing hydrogen bond interactions of $Apollo_{TBM}$ peptide with $TRF2_{TRFH}$ protein and between $TIN2_{TBM}$ and $TRF1_{TRFH}$ or $TRF2_{TRFH}$ protein, it was observed that the binding pocket of $TIN2_{TBM}$ peptide is deeper and residues present in that region form stronger

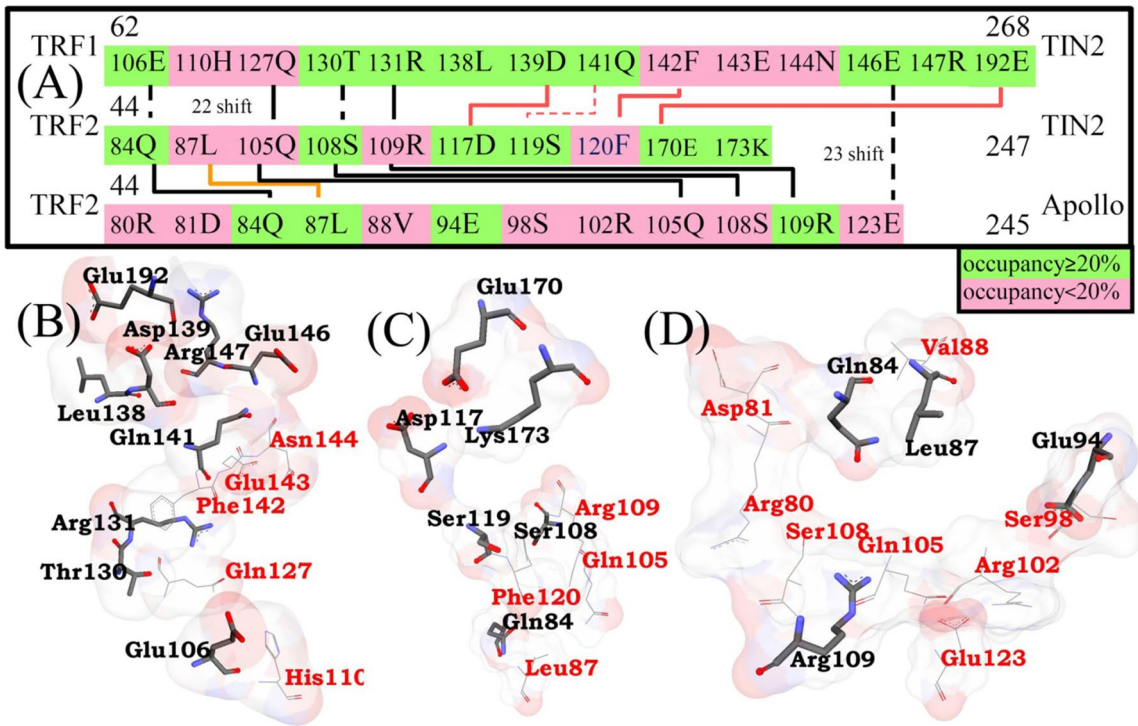

Fig. 5 Binding site residues of TRF protein with their respective peptides. **a** Protein residues involved in hydrogen bonding (acceptor donor distance ≤3.5 Å) of $TRF1_{TRFH}$ and $TRF2_{TRFH}$ protein with $TIN2_{TBM}$ or $Apollo_{TBM}$ peptides, respectively. In **b** $TRF1_{TRFH}$-$TIN2_{TBM}$ complex **c** $TRF2_{TRFH}$-$TIN2_{TBM}$ complex, and **d** $TRF2_{TRFH}$-$Apollo_{TBM}$ complex, residues involved in hydrogen bonding having occupancy ≥20 % are presented in *sticks* and labeled in *black*, and residues involved in hydrogen bonding having occupancy <20 % are presented in *line* and labeled in *red*. (Colors of atoms: carbon in *grey*, nitrogen in *blue*, and oxygen in *red*). Lines-legend for **a** *black line* represents common residues of protein–peptide interaction, *black dashed line* not exact match but complementary interactions, *red line* represent common residues involved in both $TRF1_{TRFH}$-$TIN2_{TBM}$ and $TRF2_{TRFH}$-$TIN2_{TBM}$ complexes and *red dashed line* represents not exactly matching but complementary interactions. The *orange line* shows residues involved in H-bond interaction with peptide in both $TRF2_{TRFH}$-$TIN2_{TBM}$ and $TRF2_{TRFH}$-$Apollo_{TBM}$ complexes

hydrogen bonds (based on the number of H-bonds formed) compared to the $Apollo_{TBM}$ peptide.

The fast motion, high degree of freedom, and various different conformations displayed by each peptide (or individual residues of a peptide) during the MD simulations were analyzed via their hydrogen bond networks. Hydrogen bond networks were identified by tracing interactions in terms of occupancy between the atoms acting as hydrogen bond donors or acceptors in each protein–peptide complex. Many temporary hydrogen bonds were observed between TRF protein and each peptide, but only stable interactions having occupancy ≥20 %, were considered (Fig. S5, S6, and S7). Figures 5, 6, and Table 1 depict detailed interactions between individual residues of $TRF1_{TRFH}$ and $TRF2_{TRFH}$ proteins with their respective partners $TIN2_{TBM}$ or $Apollo_{TBM}$. The most conserved and strongest hydrogen bond network involves the side chain of 106GLU and 84GLN in $TRF1_{TRFH}$-$TIN2_{TBM}$ and $TRF2_{TRFH}$-$TIN2_{TBM}$/$TRF2_{TRFH}$-$Apollo_{TBM}$ complex (occupancy ≥20 %) (Fig. 5a, e), and this correlates with the work of Chen et al. (2008). Other stably H-bonding residues (occupancy ≥20 %) common to $TRF1_{TRFH}$ and $TRF2_{TRFH}$ proteins (considering the 22 amino acid shift of numbering in $TRF1_{TRFH}$ to that of $TRF2_{TRFH}$) in their interaction with $TIN2_{TBM}$ were the side chains of 130THR/108SER, the main and side chain of 139ASP/117ASP, and the main chain of 141GLN/119SER (Table 1) (Fig. 5a).

Beside the differences in the interactions of the respective peptides–protein pairs, there were some similarities as well. Among long-lasting interactions, 127GLN/105GLN, 131ARG/109ARG, 139ASP/117ASP, 142PHE/120PHE and 192GLU/170GLU were common functional residues of $TRF1_{TRFH}$/$TRF2_{TRFH}$ proteins making contact with the $TIN2_{TBM}$ peptide (occupancy <20 %). Comparing the functional residues of $TRF2_{TRFH}$ in $TRF2_{TRFH}$-$TIN2_{TBM}$ and $TRF2_{TRFH}$-$Apollo_{TBM}$ complexes, five (84GLN, 87LEU, 105GLN, 108SER, and 109ARG) were commonly involved in intermolecular hydrogen bond formation with the bound peptide ($TIN2_{TBM}$ or $Apollo_{TBM}$). Analysis of the most conserved and common functional residues in $TRF1_{TRFH}$ and $TRF2_{TRFH}$ proteins indicated the active binding region for the peptides (Fig. 5). Thus modulating or blocking these

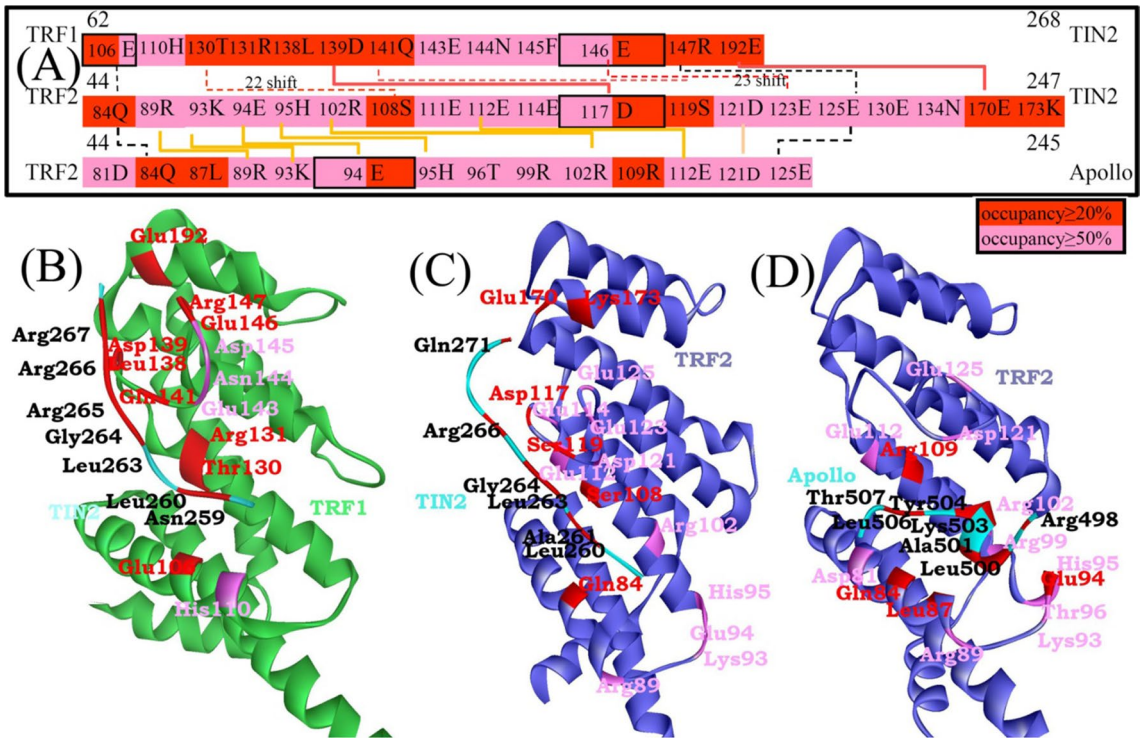

Fig. 6 **a** Residues of protein ($TRF1_{TRFH}$ and $TRF2_{TRFH}$) that are consistently involved in protein–peptide (*red*) and protein–water interactions (*violet*), **b–d** show orientation of TRF protein during hydrogen bonding with peptide and water. ($TRF1_{TRFH}$/$TRF2_{TRFH}$ protein is colored in *green/blue*, peptide is in *blue* and H-bond forming residues of peptide or protein are in *red*, residues from the peptide are marked in *black*, and residues of the protein interacting with water are in *violet*). Lines-legend for **a** *black dashed line* represents common residues of protein involved in the H-bond interactions with peptide or water in all three systems and represents also not exact match but complementary interactions. The *red lines* represent common residues involved in hydrogen bond interaction in both $TRF1_{TRFH}$-$TIN2_{TBM}$ and $TRF2_{TRFH}$-$TIN2_{TBM}$ complexes and *red dashed line* represent not exact match but complementary interactions. *Orange line* shows residues involved in H-bond interaction with peptide or water in both $TRF2_{TRFH}$-$TIN2_{TBM}$ and $TRF2_{TRFH}$-$Apollo_{TBM}$ complexes

Table 1 Hydrogen bond occupancy between donor and acceptor atoms of TRF proteins with their respective peptides ($TIN2_{TBM}$ or $Apollo_{TBM}$)

$TRF1_{TRFH}$-$TIN2_{TBM}$			$TRF2_{TRFH}$-$TIN2_{TBM}$			$TRF2_{TRFH}$-$Apollo_{TBM}$		
Protein	Peptide	Occ.	Protein	Peptide	Occ.	Protein	Peptide	Occ.
106GLU-S	260LEU-M	24.95	84GLN-S	261ALA-M	26.15	84GLN-S	501ALA-M	27.84
130THR-S	260LEU-M	43.41	84GLN-S	260LEU-M	20.96	84GLN-S	506LEU-M	20.86
131ARG-S	259ASN-M	29.64	108SER-S	260LEU-M	26.05	87LEU-M	500LEU-M	27.35
138LEU-M	266ARG-S	26.75	117ASP-M	266ARG-M	43.21	94GLU-S	503LYS-S	69.46
139ASP-S	265ARG-S	39.92	117ASP-S	266ARG-S	54.59	94GLU-S	504TYR-S	55.99
139ASP-M	266ARG-M	47.01	119SER-M	263LEU-M	23.75	109ARG-S	505LEU-M	38.52
139ASP-S	267ARG-S	28.74	119SER -M	264GLY-M	41.22	109ARG-S	506LEU-M	20.76
141GLN-M	264GLY-M	37.62	119SER-M	264GLY-M	33.93			
141GLN-M	263LEU-M	26.25	170GLU-S	ARG266-S	86.83			
146GLU-S	267ARG-S	30.74	173LYS-S	GLN271-M	23.35			
147ARG-M	266ARG-S	47.01						
192GLU-S	266ARG-S	84.83						
192GLU-S	267ARG-S	21.76						

Occ. % occupancy of interaction over 1000 ns, *S* side chain, *M* main chain, life span (occupancy less than 20 % is not shown in table)

Table 2 Average distances (Å) between atoms of peptide and protein obtained from molecular dynamics simulations of protein–peptide complexes

$TRF1_{TRFH}$-$TIN2_{TBM}$			$TRF2_{TRFH}$-$TIN2_{TBM}$			$TRF2_{TRFH}$-$Apollo_{TBM}$		
Peptide/atoms	Protein/atoms	Average distance (Å)	Peptide/Atoms	Protein/atoms	Average distance (Å)	Peptide/atoms	Protein/atoms	Average distance (Å)
262P/CG	142F/CZ	4.108	262P/CG	120F/CZ	4.433	508P/CG	120F/CD2	4.540
260L/CG	86L/CG	7.677	260L/CG	80R/CB	6.298	506L/CG	80R/CG	5.250
260L/CG	102R/CG	4.606	260L/CG	83M/CG	6.053	506L/CG	83M/CE	6.138
260L/CG	105A/CB	5.341	260L/CG	84Q/CD	5.026	506L/CG	84Q/CD	4.752
260L/CG	106E/CB	4.772	260L/CG	87L/CD1	5.369	506L/CG	87L/CD1	4.826
260L/CG	109I/CD	4.625	260L/CG	104 M/CG	4.684	506L/CG	104M/CG	4.594
260L/CG	126C/CB	5.108	260L/CG	105Q/CG	6.036	506L/CG	105Q/CG	6.024
260L/CG	127Q/CG	5.066	260L/CG	108S/CB	5.960	506L/CG	108S/CB	5.892
260L/CG	130T/CG2	4.923	258F/CE2	87L/CD2	6.283	504Y/CE2	101L/CD1	4.574
258F/CE1	109I/CG2	5.981	258F/CE2	101L/CD1	4.777	504Y/CE2	102R/CZ	3.787
258F/CE1	115L/CD1	6.025				501A/CA	87L/CB	4.037
258F/CE1	120L/CD1	6.329				501A/CA	88V/CG1	6.036
258F/CE1	123I/CG2	4.945				500L/CA	87L/CD2	5.887
258F/CE1	124Y/CE1	6.731				500L/CA	88V/CG1	7.755
						500L/CA	91L/CD2	8.436
						500L/CA	94E/CG	7.303
						500L/CA	97V/CG2	8.762
						500L/CA	101L/CG	8.141

Residues of protein-forming hydrophobic interactions in crystallographic structures by Chen et al. (2008) were selected for calculating distance between atoms

residues of TRF proteins may help to modulate the activity of TRF proteins interacting with telomeric DNA or other shelterin proteins.

Molecular dynamics vs. experimental data

Molecular dynamics results complement well the X-ray models of Chen et al. (2008) and also the study of the $Apollo_{TBM}$ derived $TRF2_{TRFH}$ binder by DiMaro et al. (2014). However, our MD simulations extend understanding of the systems based on X-ray studies alone. In particular, despite the similarities between molecular dynamics and experimental data, there were some interactions in $TRF1/2_{TRFH}$–peptide complexes only observed by MD.

Quantitative assessments of interacting residues from crystallographic studies (Chen et al. 2008)

Studying dynamic behavior of the system is usually useful, and in many cases indispensable to supplement static X-ray structures, since different conformational changes of protein can be traced in molecular dynamics. Thus, theoretical studies and experimental data complement one another: results obtained from molecular dynamics calculations provide a quantitative assessment of interactions described in the structural work of Chen et al. (2008). The list of residues from the $TRF1_{TRFH}$ and $TRF2_{TRFH}$ proteins interacting with $TIN2_{TBM}$ or $Apollo_{TBM}$ peptide in the work of Chen et al. (2008), forming hydrophilic or hydrophobic interactions, is presented in Tables 2 and 3. In particular, H-bonding occupancies were traced over 1000 ns of MD simulation time along with the average distance for hydrophobic interactions (Table 2) making a comparative analysis of data obtained from experimental and MD studies (Table 3).

As shown in Table 2, and Figure S8, S9, and S10, only a few hydrophobic interactions show persistent short distances and most of the residues exhibit similar interactions in both MD and X-ray studies. In the $TRF1_{TRFH}$-$TIN2_{TBM}$ complex, residue 130THR of TRF1 makes a dominant hydrophilic interaction with peptide $TIN2_{TBM}$ and this interaction lasts for 43.41 % of the total MD simulation time. Residue 130THR of $TRF1_{TRFH}$ domain of TRF1 protein is also one of the most interacting residues with $TIN2_{TBM}$ peptide in terms of occupancy whereas in crystallographic studies of Chen et al. (2008) this 130THR residue of $TRF1_{TRFH}$ protein forms only hydrophobic interactions; similar differences have been observed for the $TRF2_{TRFH}$-$TIN2_{TBM}$ and $TRF2_{TRFH}$-$Apollo_{TBM}$ complexes. Residue 108SER in $TRF2_{TRFH}$ protein ($TRF2_{TRFH}$-$TIN2_{TBM}$) which

Table 3 List of TRF protein residues interacting with $TIN2_{TBM}$ or $Apollo_{TBM}$ peptide as described in work of Chen et al. (2008) forming hydrophilic and hydrophobic interactions and their occupancy time (H-bonds in hydrophilic and hydrophobic, and additionally average distance from Table 2 for hydrophobic interactions) obtained from 1000 ns of MD simulation time

$TRF1_{TRFH}$-$TIN2_{TBM}$		$TRF2_{TRFH}$-$TIN2_{TBM}$		$TRF2_{TRFH}$-$Apollo_{TBM}$	
Hydrophilic (Occup.)	Hydrophobic (Occup.)/AV	Hydrophilic (Occup.)	Hydrophobic (Occup.)/AV	Hydrophilic (Occup.)	Hydrophobic (Occup.)/AV
106GLU (24.95 %)	86LEU (0.00 %)/(7.677 Å)	84GLN (26.15 %)	80ARG (2.00 %)/(6.298 Å)	84GLN (27.84 %)	80ARG (5.08 %)/(5.250 Å)
127GLN (10.18 %)	102ARG (2.5 %)/(4.606 Å)	109ARG (3.69 %)	83MET (0.00 %)/(6.053 Å)	94GLU (69.46 %)	83MET (0.10 %)/(6.138 Å)
131ARG (29.64 %)	105ALA (0.00 %)/(5.341 Å)	115LEU (0.00 %)	84GLN (26.15 %)/(5.026 Å)	98SER (8.47 %)	84GLN (27.84 %)/(4.752 Å)
138LEU (26.75 %)	106GLU (24.95 %)/(4.772 Å)	117ASP (54.59 %)	87LEU (1.60 %)/(5.369 Å)	102ARG (4.69 %)	87LEU (27.35 %)/(4.037 Å)
139ASP (47.01 %)	109ILE (0.80 %)/(4.625 Å)	119SER (41.22 %)	101LEU (0.10 %)/(4.777 Å)	105GLN (10.77 %)	88VAL (2.69 %)/(6.036 Å)
141GLN (37.62 %)	115LEU (0.10 %)/(6.025 Å)	120PHE (11.38 %)	104MET (0.00 %)/(4.684 Å)	109ARG (38.52 %)	91LEU (0.90 %)/(8.436 Å)
142PHE (12.08 %)	120LEU (0.00 %)/(6.329 Å)	126GLU (0.00 %)	105GLN (8.68 %)/(6.036 Å)	119 SER (0.40 %)	94GLU (69.46 %)/(7.303 Å)
146GLU (30.74 %)	123ILE (0.00 %)/(4.945 Å)	170GLU (86.83 %)	108SER (26.05 %)/(5.960 Å)		97VAL (0.00 %)/(8.762 Å)
ARG147 (47.01 %)	124TYR (0.20 %)/(6.731 Å)		120PHE (11.38 %) (4.433 Å)		101LEU (0.00 %)/(4.574 Å)
192GLU (84.83 %)	126CYS (0.10 %)/(5.108 Å)				102ARG (4.69 %)/(3.787 Å)
	127GLN (10.18 %)/(5.066 Å)				104MET (0.00 %)/(4.594 Å)
	130THR (43.41 %)/(4.923 Å)				105GLN (10.77 %)/(6.024 Å)
	142PHE (12.08 %)/(4.108 Å)				108SER (4.69 %)/(5.892 Å)
					120PHE (0.50 %)/(4.540 Å)

Occup. % occupancy of interaction over 1000 ns, *AV* average distance

performs the role of 130THR in $TRF1_{TRFH}$-$TIN2_{TBM}$, and 87LEU in $TRF2_{TRFH}$-$Apollo_{TBM}$ show dominant hydrophilic interactions, whereas they form only hydrophobic interactions in the crystal structured of Chen et al. (2008).

Molecular dynamics explaining mutational studies of Chen et al. (2008)

Differences in hydrophilic and hydrophobic interactions could be considered very important as a basis for mutating the residues forming strong hydrophilic interactions to modulate interaction of TRF proteins with telomeric DNA and other shelterin proteins. Additionally, detailed information about a particular type (protein–peptide) of interaction can be used for pharmacophore elaboration and the design of modulators. Our observation is consistent with mutational studies of Chen et al. (2008) in which $TIN2_{TMB}$LEU260ALA prevented its binding to $TRF1_{TRFH}$. Indeed, if 130THR of $TRF1_{TRFH}$ binds with 260LEU of $TIN2_{TMB}$ only through hydrophobic interactions then replacing LEU for ALA should not cause such a difference; but considering our MD results suggest a strong H-bond of 260LEU with 130THR of $TRF1_{TRFH}$, distortions after mutation of 260LEU to 260ALA would indeed explain the lack of binding of $TIN2_{TMB}$LEU260ALA with $TRF1_{TRFH}$ protein.

Molecular dynamics results determined some extra protein–peptide interactions apart from those observed in the experimental study of Yong Chen et al. (2008). Chen et al. (2008) found that 127GLN of $TRF1_{TRFH}$ formed a hydrophilic interaction with TIN2, whereas in the MD simulation this residue was not observed to form a dominant hydrophilic interaction. Similarly in the $TRF2_{TRFH}$-$TIN2_{TBM}$ complex MD residues 105GLN, 109ARG, 115LEU, and

126GLU of $TRF2_{TRFH}$ did not form hydrophilic interactions with $TIN2_{TBM}$, but experimentally they were found to (Chen et al. 2008). By contrast, 173LYS of $TRF2_{TRFH}$ formed an H-bond with the $TIN2_{TBM}$ peptide in the MD analysis but this interaction was not found in experimental studies (Chen et al. 2008). For $TRF2_{TRFH}$-$Apollo_{TBM}$ complex, experimental data (Chen et al. 2008) suggest that 98SER, 102ARG, 105GLN, and 119SER of $TRF2_{TRFH}$ made hydrophilic interactions with $Apollo_{TBM}$, but these interactions were not observed in the MD.

Chen et al. (2008) introduced the reverse or swapping mutants 192GLU → 192LYS/146GLU → 146ALA in $TRF1_{TRFH}$ and 173LYS → 173GLU/124ALA → 124GLU in $TRF2_{TRFH}$ and found that substitution of a negatively charged residue (192GLU) with a positively charged residue (192LYS) substantially impaired the interaction of $TRF1_{TRFH}$ with $TIN2_{TBM}$. Our MD study supports this finding as we observed the formation of a strong interaction between 192GLU of $TRF1_{TRFH}$ and 266ARG (+charged) of $TIN2_{TBM}$. A second mutation they tested in $TRF1_{TRFH}$ was 146GLU → 146ALA (Chen et al. 2008) to find that the binding of $TRF1_{TRFH}$ then remains almost the same towards $TIN2_{TBM}$ as with wild type protein. Our MD analysis again explains this finding. In the X-ray structure, 146GLU of $TRF1_{TRFH}$ interacts with both 266ARG and 267ARG of $TIN2_{TBM}$ (Chen et al. 2008) but in the MD study 146GLU interacts only with 267ARG of the peptide, whereas 266ARG of the peptide has interactions with 138LEU, 139ASP, and 147ARG of $TRF1_{TRFH}$ protein (Table 1). Since, 146GLU of protein interacts only with 267ARG of the peptide and the mutation 146GLU → 146ALA replaces residue and neutralizes its charge but does not invert its polarity, this could explain why the binding is not much changed. On the basis of our MD results, we suggest that mutating highly the interacting residues 130THR, 138LEU, 139ASP, and 192GLU of $TRF1_{TRFH}$ should give much weaker binding of TRF1 towards $TIN2_{TBM}$ (Table 1).

In $TRF2_{TRFH}$ protein, Chen et al. (2008) mutated 173LYS → 173GLU and 124ALA → 124GLU to improve binding of the protein with $TIN2_{TBM}$ (Chen et al. 2008). In our MD study, 266ARG of $TIN2_{TBM}$ has not formed any interactions either with 173LYS or 124ALA (Table 1), even though in vitro binding data after these mutations to $TRF2_{TRFH}$ show slightly improved binding of $TIN2_{TBM}$ peptide (Chen et al. 2008). This could be explained by the fact that mutating positively charged (173LYS) or hydrophobic residue (124ALA) to a negatively charged residue (173GLU and 124GLU) may have changed the overall interaction pattern of $TRF2_{TRFH}$ with $TIN2_{TBM}$ as negatively charged 173GLU and 124GLU can form polar interaction with positively charged 266ARG. Additionally, Chen et al. (2008) showed that modifying 173LYS → 173GLU in $TRF2_{TRFH}$ enhances binding of protein with peptide more than 124ALA → 124GLU. This could also be explained by our MD results, where 173LYS forms interactions with 271GLN of $TIN2_{TBM}$ whereas 124ALA of $TRF2_{TRFH}$ forms no interactions with $TIN2_{TBM}$. Furthermore, from the MD results obtained, we assume that mutating residues of $TRF2_{TRFH}$ protein that have obtained high H-bond occupancy (117ASP, 119SER, and 170GLU) with $TIN2_{TBM}$, may result in weaker binding of $TRF2_{TRFH}$ towards $TIN2_{TBM}$.

Molecular dynamics compared with studies of DiMaro et al. (2014)

Interaction analysis of $TRF2_{TRFH}$ protein with $Apollo_{TBM}$ peptide based on MD results correlate well with experimental data on an $Apollo_{TBM}$-derived $TRF2_{TRFH}$ binder (modified $Apollo_{TBM}$ peptide) (DiMaro et al. 2014). Five residues, 84GLN, 87LEU, 102ARG, 105GLN, and 108SER of the $TRF2_{TRFH}$ protein interacting with $Apollo_{TBM}$ were common to our study the work of DiMaro et al. (2014). The same set of $TRF2_{TRFH}$ residues (interacting with $Apollo_{TBM}$) showed strong interaction with the most potent interfering peptides designed on the basis of the experimental $Apollo_{TBM}$-$TRF2_{TRFH}$ structure (DiMaro et al. 2014). The interacting residues in the $TRF2_{TRFH}$-$TIN2_{TBM}$ complex were found to be almost the same as in the $TRF2_{TRFH}$-$Apollo_{TBM}$, save for two residues (119SER and 120PHE) that were common instead with the $Apollo_{TBM}$ derived peptide (DiMaro et al. 2014).

Solvent-accessible surface area (SASA)

The solvent-accessible surface area (SASA) of biomolecules and SASA change upon binding are a measure of hydrophobic interactions. SASA is generally calculated using a 'rolling ball' algorithm (Shrake and Rupley 1973). Solvent accessibility is generally divided into buried and exposed regions, indicating the low and high accessibility of residues to solvent (Gilis and Rooman 1996). In our studies, contact solvent-accessible area was calculated from MD trajectories for each MD frame (Fig. 7). The SASA values for protein–peptide ($TRF1_{TRFH}$-$TIN2_{TBM}$, $TRF2_{TRFH}$-$TIN2_{TBM}$, and $TRF2_{TRFH}$-$Apollo_{TBM}$) complexes were calculated according to the formula: <*Contact SASA*> = <*SASA of Receptor protein alone*> + <*SASA of Ligand protein alone*> − <*SASA of docked protein complex*> .

Analyzing SASA values of $TRF1_{TRFH}$ and $TRF2_{TRFH}$ protein alone and in complex with the peptide we observed that all three systems have an average solvent-accessible surface area in the range ~120–140 nm^2 (Fig. 7a–c). The $TIN2_{TBM}$ peptide from $TRF1_{TRFH}$-$TIN2_{TBM}$ has a higher SASA compared to $TIN2_{TBM}$ in the $TRF2_{TRFH}$-$TIN2_{TBM}$ complex, while $TIN2_{TBM}$ in $TRF2_{TRFH}$-$TIN2_{TBM}$

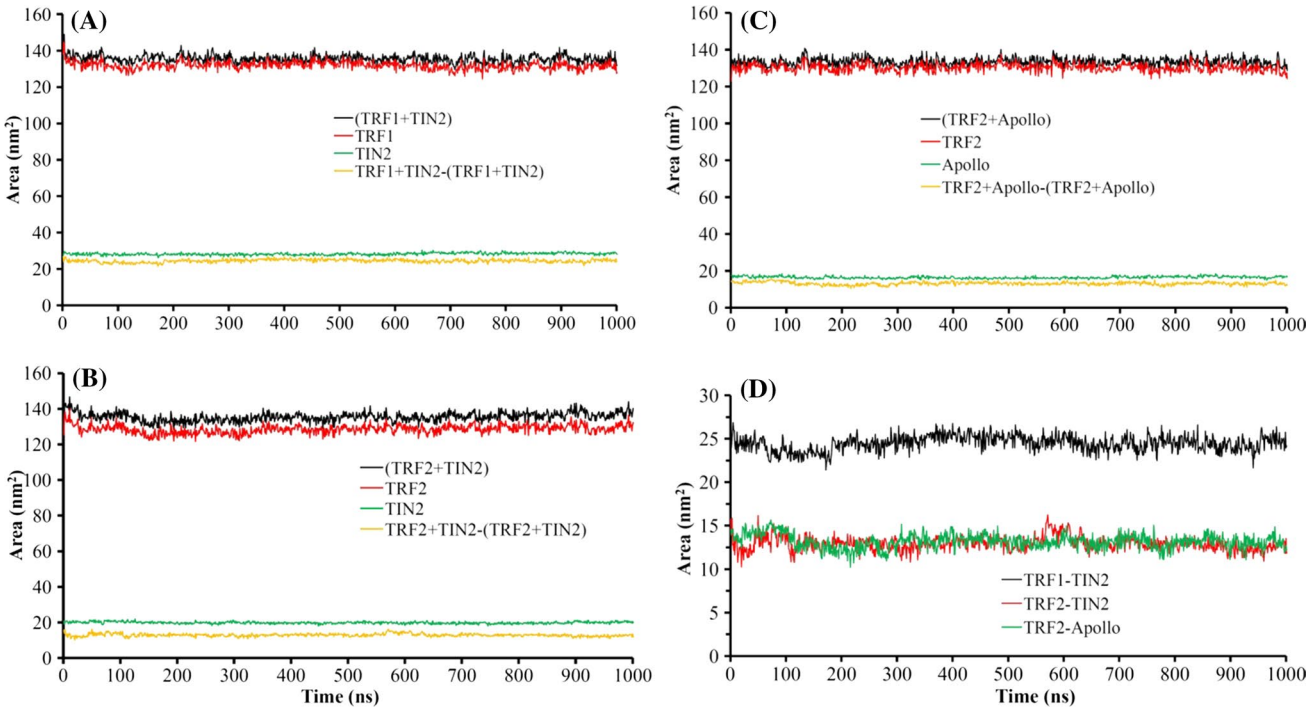

Fig. 7 **a–c** Solvent-accessible surface area (SASA) as well as contact SASA of TRF1, TRF2, TIN2 and Apollo alone (individually taken from protein–peptide complexes) and in complete protein–peptide complexes. **d** The contact solvent-accessible surface area (SASA) of the interacting region in both, protein and peptide from $TRF1_{TRFH}$-$TIN2_{TBM}$, $TRF2_{TRFH}$-$TIN2_{TBM}$, and $TRF2_{TRFH}$-$Apollo_{TBM}$ complexes

has a higher SASA compared to $Apollo_{TBM}$ from the $TRF2_{TRFH}$-$Apollo_{TBM}$ complex (Fig. 7a–c). It seems that the $TIN2_{TBM}$ peptide behaves differently when in complex with $TRF1_{TRFH}$ or $TRF2_{TRFH}$, and a similar difference is observed with binding of $TIN2_{TBM}$ or $Apollo_{TBM}$ peptides to $TRF2_{TRFH}$ protein. Analysis of SASA (Fig. 7) correlates well with RMSD (Fig. 2) data.

Despite differences in the surface area of $TIN2_{TBM}$ and $Apollo_{TBM}$ in complex with $TRF2_{TRFH}$ protein, the $TRF2_{TRFH}$ protein in complex with two different peptides ($TIN2_{TBM}$ or $Apollo_{TBM}$) exhibited a similar solvent-accessible area in each case (~12–15 nm^2). In contrast to $TRF2_{TRFH}$, the $TRF1_{TRFH}$-$TIN2_{TBM}$ complex has a higher contact solvent-accessible area of ~23–27 nm^2 (Fig. 7d), indicating that binding of $TIN2_{TBM}$ to $TRF1_{TRFH}$ has more H-bond forming properties than $TRF2_{TRFH}$-$TIN2_{TBM}$/$Apollo_{TBM}$. Moreover, an increase or decrease in the solvent-accessible surface area describes a change in the solvent-exposed residues of protein–peptide complexes. Comparing contact SASA data of $TRF1_{TRFH}$ with the H-bond interactions with water (Fig. S11 and Table S1), we observe that protein regions interacting with peptide show less interaction with water, as might be expected. This suggests that $TRF1_{TRFH}$ protein residues interacting with peptides (Figs. 4, 5, 6; Table 1) form more stable hydrogen bond interactions than with water. The SASA results support our observation that $TIN2_{TBM}$ has a well-defined binding mode with $TRF1_{TRFH}$ as compared to with $TRF2_{TRFH}$ (Figs. 2, 4, 5) and suggests although these proteins are structurally similar they are functionally very different. The contact solvent-accessible surface area (Fig. 7d) also explains the observed hydrophobic interactions and their contribution to the free energy of peptide binding, which is bigger for the $TRF1_{TRFH}$-$TIN2_{TBM}$ than $TRF2_{TRFH}$-$TIN2_{TBM}$ complex. This hydrophobic effect and the possibility that $TRF1_{TRFH}$ forms more H-bonding interactions indicate that this protein has formed a well-defined binding mode with $TIN2_{TBM}$ compared to $TRF2_{TRFH}$.

Stable hydrogen bond contacts between TRF proteins and water molecules

$TRF1_{TRFH}$ and $TRF2_{TRFH}$ residues showing interaction with $TIN2_{TBM}$ or $Apollo_{TBM}$ were considered for protein-water interaction analysis, using $TRF1_{TRFH}$ residues 104–112 and 125–155, and $TRF2_{TRFH}$ residues: 80–129 and 130–135. Protein-water interactions help to maintain a flexible conformation required for protein recognition (Bone and Pethig 1985; Takano et al. 2003) and were analyzed to understand the behavior of TRF proteins since protein residues interacting more (or equally) with water than with bound peptides are available to interact with other

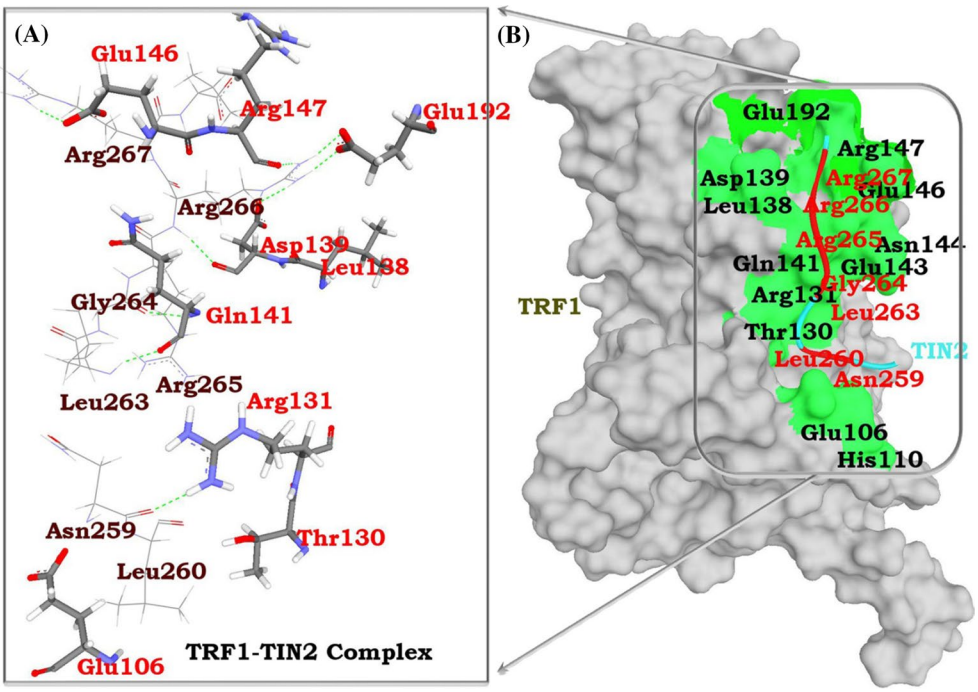

Fig. 8 Intermolecular hydrogen bonding pattern of TRF proteins with peptides obtained from the end of the simulation. **a** $TRF1_{TRFH}$ protein is represented as *sticks* and $TIN2_{TBM}$ peptide is shown as *lines*. Hydrogen bonds are presented as *green dashed lines*. Atoms colored in *red*, *blue*, *grey*, and *silver* are oxygen, nitrogen, carbon and hydrogen atoms respectively. **b** $TRF1_{TRFH}$ protein is shown as surface representation in *grey color* and peptide as *solid ribbon* representation in *blue color*. *Red color* region with labeled residues of peptide and *green color* region with *black* labeled residues of protein show the interacting residues of protein–peptide complex

small molecules (peptides/proteins) by the replacement of H-bond interactions with water by contacts with small molecules or peptides/proteins.

Fast residue motion during simulations led to numerous water molecule encounters, but most were temporary and made a minor contribution. To account for this, we only selected H-bond interactions lasting at least 50 % of the simulation time. Despite differences in the interaction pattern of protein with peptide in all three protein–peptide complexes, there were some similarities found in protein-water interactions, with ten residues found to be common to all three systems ($TRF1_{TRFH}$-$TIN2_{TBM}$, $TRF2_{TRFH}$-$TIN2_{TBM}$, and $TRF2_{TRFH}$-$Apollo_{TBM}$). Thirty-six $TRF2_{TRFH}$ residues interacting with water molecules were replicated in simulations with $TRF2_{TRFH}$-$TIN2_{TBM}$ or $TRF2_{TRFH}$-$Apollo_{TBM}$ (Fig. S11). Water molecules made different kinds of contacts with $TRF1_{TRFH}$ protein, contacting the main or side chains of six residues: 106GLU, 110HIS, 143GLU, 144ASN, 145ASP, and 146GLU. Nine residues (89ARG, 93LYS, 94GLU, 95HIS, 102ARG, 112GLU, 121ASP, 123GLU, and 125GLU) of $TRF2_{TRFH}$ protein in the two different complexes were commonly involved in water-protein interactions with occupancy > 50 % (Fig. S11 and Table S1). Among the 12 best hydrogen bond forming (with peptide and water) residues of $TRF1_{TRFH}$, two residues (106GLU and 146GLU) were involved in both protein–peptide and protein-water interactions (Fig. 6a). From 17 highly interacting residues of $TRF2_{TRFH}$ protein with water and peptide in the $TRF2_{TRFH}$-$TIN2_{TBM}$ complex, nine residues (84GLN, 89ARG, 93LYS, 94GLU, 95HIS, 102ARG, 112GLU, 121ASP, and 125GLU) were common with the $TRF2_{TRFH}$-$Apollo_{TBM}$ complex (Fig. 6a).

Comparing interactions of TRF proteins with $TIN2_{TBM}$ or $Apollo_{TBM}$ peptides and water, we observed that most of the residues forming weak interaction with peptide showed stable interaction with water molecules (Figs. 5a, 6a, and S11). Although the $TRF2_{TRFH}$ protein has a lower SASA compared to the $TRF1_{TRFH}$ protein, it has more interactions with water molecules than $TRF1_{TRFH}$ (Fig. 7); conversely $TRF2_{TRFH}$ forms less contact with the $TIN2_{TBM}$ peptide (Figs. 4, 6; Table 1 and S1). Since, the $TRF2_{TRFH}$ protein has more interactions with water and comparatively less with $TIN2_{TBM}$ compared to $TRF1_{TRFH}$, we conclude that $TRF2_{TRFH}$ has more capability to interact with different peptides (e.g., $TIN2_{TBM}$ or $Apollo_{TBM}$) than $TRF1_{TRFH}$, with a less well defined binding site.

Interaction pattern of $TRF1_{TRFH}$ and $TRF2_{TRFH}$ protein with peptide

Overall, we found that the $TRF2_{TRFH}$ protein has a different network of interacting residues with both $TIN2_{TBM}$ and $Apollo_{TBM}$ peptides (Fig. 6c, d, S12, and S13) compared to TRF1. Although the conformation of the $TIN2_{TBM}$ peptide bound to $TRF1_{TRFH}$ or $TRF2_{TRFH}$ is almost the same (Figs. 5, 8, and S12), slight changes in conformation could be responsible for a significant difference in peptide binding affinity (Fig. 9 and S14).

Different residues performing the same interactional function, and the formation of H-bond interactions

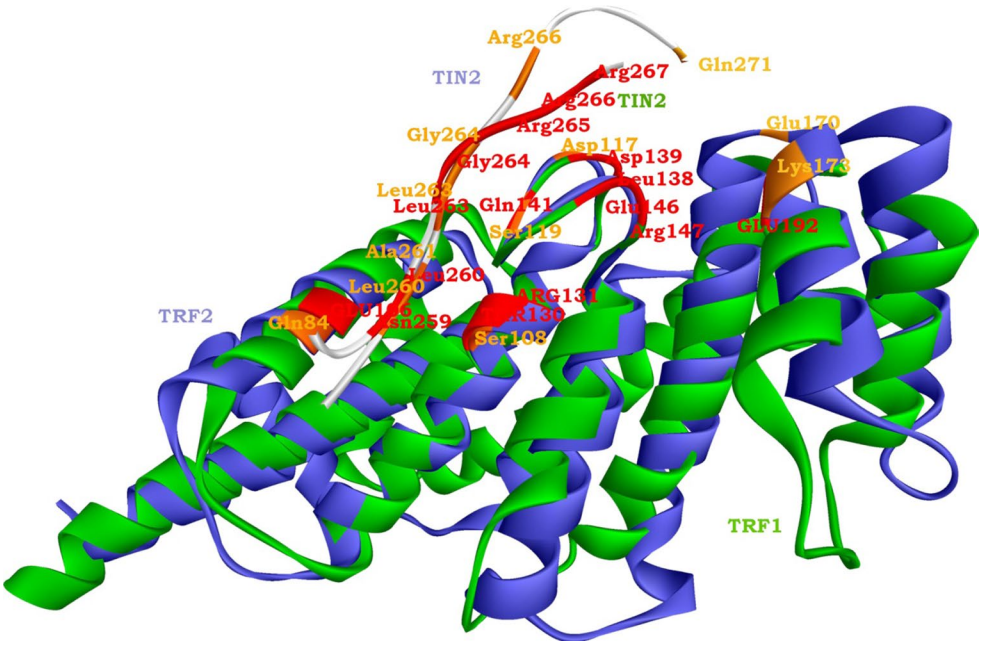

Fig. 9 $TRF1_{TRFH}$ (*green* color)-$TIN2_{TBM}$ (*silver* representation and label TIN2 in *green*) superimposed on $TRF2_{TRFH}$ (*blue color*)-$TIN2_{TBM}$ (*silver* representation and label TIN2 in *blue*) structure. Protein and peptide is represented as *solid ribbon* and interacting residues of $TRF1_{TRFH}$ with peptide are shown in *red color* and interacting residues of $TRF2_{TRFH}$ protein with peptide are shown in *orange color*, and the same pattern is followed for the peptide

with target peptides, were found in all three complexes ($TRF1_{TRFH}$-$TIN2_{TBM}$, $TRF2_{TRFH}$-$TIN2_{TBM}$/$Apollo_{TBM}$), involving 106GLU/84GLN, 130THR/108SER, and 141GLN/119SER (Figs. 5, 6). From the $TIN2_{TBM}$ peptide perspective, we observed that though it has different SASA values and water interacting residues in both TRF protein complexes, it makes an almost identical H-bond interacting network with $TRF1_{TRFH}$ and $TRF2_{TRFH}$ protein, saving some interactions specific to $TRF1_{TRFH}$ or $TRF2_{TRFH}$ (Fig. 6b, c). Only the residues 138LEU (26.75 %), 146GLU (30.74 %), and 147ARG (47.01 %) of $TRF1_{TRFH}$ were only found to interact with $TIN2_{TBM}$ with an occupancy ≥20 %. In the $TRF2_{TRFH}$-$TIN2_{TBM}$ and $TRF2_{TRFH}$-$Apollo_{TBM}$ complexes, the $TRF2_{TRFH}$ residues 117ASP (54.59 %), 119SER (23.75 %), 170GLU (86.83 %), and 173LYS (23.35 %) were observed making interaction only with $TIN2_{TBM}$, whereas only residues 94GLU (69.46 %) and 109ARG (38.52 %) made contacts with occupancy ≥20 % to $Apollo_{TBM}$. These differences in the dominant interacting residues for $TRF1_{TRFH}$ and $TRF2_{TRFH}$ proteins with their respective ligands may regulate the binding of TRF proteins to TIN2 and Apollo.

Conclusions

Predicting protein–peptide binding interactions is one of the most challenging problems in computational structural biology due to the large number of peptide degrees of freedom. Nevertheless, such interactions are selective and important for protein–peptide recognition, as in our case where they are responsible for the proper function of the shelterin complex. In summary, here an MD study demonstrated how the contribution of "classically" observed residues and motifs (of TRF_{TRFH} proteins) to peptide binding can be explained at a molecular level in terms of interaction networks, conferring specific dynamical characteristics on TRF_{TRFH} when in contact with distinct shelterin components (peptides).

We traced structural and dynamical aspects of $TIN2_{TBM}$ or $Apollo_{TBM}$ peptide interactions with $TRF1_{TRFH}$ or $TRF2_{TRFH}$, and thereby quantitatively assessed interactions described in experimental data (Chen et al. 2008). Comparison to experimental data (Chen et al. 2008; DiMaro et al. 2014) enabled understanding of the basis of previous observations in terms of a dynamic binding model. Some TRF_{TRFH} protein residues [130THR ($TRF1_{TRFH}$-$TIN2_{TBM}$), 108SER ($TRF2_{TRFH}$-$TIN2_{TBM}$), and 87LEU ($TRF2_{TRFH}$-$Apollo_{TBM}$)] which showed dominant hydrophilic interaction with bound peptide in the MD study were thought to form only dominant hydrophobic interactions on the basis of crystal structures (Chen et al., 2008). We have suggested that mutating interacting residues 130THR, 138LEU, and 139ASP and 192GLU of $TRF1_{TRFH}$ protein should give much weaker binding towards $TIN2_{TBM}$. Similarly, mutating residues of $TRF2_{TRFH}$ protein that have high H-bond occupancy (117ASP, 119SER, and 170GLU) with $TIN2_{TBM}$ peptide in MD may result in weaker binding than mutants of 173LYS and 124ALA (Chen et al. 2008) in $TRF2_{TRFH}$ protein.

Most of the residues forming only weak interactions with bound peptide had stable interactions with water molecules. Though $TRF2_{TRFH}$ protein has less SASA area compared to $TRF1_{TRFH}$, it has obtained more interaction with

water molecules than $TRF1_{TRFH}$ protein, and conversely $TRF2_{TRFH}$ forms less stable H-bond contacts with peptide ($TIN2_{TBM}$) than $TRF1_{TRFH}$ protein. This observation suggests that though $TRF1_{TRFH}$ and $TRF2_{TRFH}$ are structurally similar, they are functionally different and their homologous molecular recognition surfaces have distinct specificities. Since $TRF2_{TRFH}$ forms more interactions with water and comparatively less with $TIN2_{TBM}$ compared to $TRF1_{TRFH}$, we conclude that $TRF2_{TRFH}$ has a greater capacity to interact with different peptides (e.g., $TIN2_{TBM}$ or $Apollo_{TBM}$) than $TRF1_{TRFH}$.

Data obtained from our MD study have given a deeper understanding of the molecular interactions and dynamics of $TRF1/2_{TRFH}$ proteins with other shelterin components, and thus an elaborated pharmacophore model. The shelterin proteins $TRF1_{TRFH}$ and $TRF2_{TRFH}$ function not only to protect telomeres but also homeostatically to maintain telomere length, which is associated with tumorigenesis and inversely correlates with aging (deLange 2005). TRF proteins are potential chemotherapeutic targets because telomeres in cancer cells are usually shorter and more fragile than in regular cells (Diehl et al. 2011). According to our MD analysis, a small number of TRF–peptide interactions provide for specific protein–peptide complex formation, indicating a basis for designing compounds modulating telomere machinery and for anticancer therapy.

Acknowledgments The authors are thankful to the Academic Computer Centre CYFRONET (PL-Grid Infrastructure), Krakow (Poland), for providing hardware and software resources with which molecular dynamics calculations were performed.

References

Arfken G (1985) the method of steepest descents. Mathematical methods for physicists, (ed) Orlando: Academic Press, Vol. 3. pp 428–436

Baumann P, Cech T (2001) Pot1, the putative telomere end-binding protein in fission yeast and humans. Science 292:1171–1175

Bianchi A, Smith S, Chong L, Elias P, deLange T (1997) TRF1 is a dimer and bends telomeric DNA. EMBO J 16:1785–1794

Bianchi A, Stansel R, Fairall L, Griffith J, Rhodes D, deLange T (1999) TRF1 binds a bipartite telomeric site with extreme spatial flexibility. EMBO J 18:5735–5744

Bidzinska J, Baginski M, Skladanowski A (2014) Novel anticancer strategy aimed at targeting shelterin complexes by the induction of structural changes in telomeric DNA: hitting two birds with one stone. Curr Cancer Drug Targets 14:201–216

Bjelkmar P, Larsson P, Cuendet M, Hess B, Lindahl E (2010) Implementation of the CHARMM force field in GROMACS: analysis of protein stability effects from correction maps, virtual interaction sites, and water models. J Chem Theory Comput 6:459–466

Bone S, Pethig R (1985) Dielectric studies of protein hydration and hydration-induced flexibility. J Mol Biol 181:323–326

Broccoli D, Smogorzewska A, Chong L, deLange T (1997) Human telomeres contain two distinct Myb-related proteins, TRF1 and TRF2. Nat Genet 17:231–235

Bussi G, Donadio D, Parrinello M (2007) Canonical sampling through velocity rescaling. J Chem Phys 126:014101

Chen Y, Yang Y, Overbeek M, Donigian J, Baciu P, deLange T, Lei M (2008) A shared docking motif in TRF1 and TRF2 used for differential recruitment of telomeric proteins. Science 319:1092–1096

Chuang H, Chen C, Huang C, Fang F, Tsai H, Chien C (2011) Reduced expression of TRF1 is associated with tumor progression and poor prognosis in oral squamous cell carcinoma. Exp Ther Med 2:63–67

Court R, Chapman L, Fairall L, Rhodes D (2005) How the human telomeric proteins TRF1 and TRF2 recognize telomeric DNA: a view from high-resolution crystal structures. EMBO Rep 6:39–45

Dagliyan O, Proctor E, D'Auria K, Ding F, Dokholyan N (2011) Structural and dynamic determinants of protein–peptide recognition. Structure 19:1837–1845

Darden T, York D, Pedersen L (1993) Particle mesh Ewald: an N·log (N) method for Ewald sums in large systems. J Chem Phys 98:10089–10092

deLange T (2005) Shelterin: the protein complex that shapes and safeguards human telomeres. Genes Dev 19:2100–2110

Diehl M, Idowu M, Kimmelshue K, York T, Jackson-Cook C, Turner K, Holt S, Elmore L (2011) Elevated TRF2 in advanced breast cancers with short telomeres. Breast Cancer Res Treat 127:623–630

DiMaro S, Zizza P, Salvati E, DeLuca V, Capasso C, Fotticchia I, Pagano B, Marinelli L, Gilson E, Novellino E, Cosconati S, Biroccio A (2014) Shading the TRF2 recruiting function: a new horizon in drug development. J Am Chem Soc 136:16708–16711

Fairall L, Chapman L, Moss H, de Lange T, Rhodes D (2001) Structure of the TRFH dimerization domain of the human telomeric proteins TRF1 and TRF2. Mol Cell 8:351–361

Frescas D, deLange T (2014) TRF2-tethered TIN2 can mediate telomere protection by TPP1/POT1. Mol Cell Biol 34:1349–1362

Gilis D, Rooman M (1996) Stability changes upon mutation of solvent-accessible residues in proteins evaluated by database derived potentials. J Mol Biol 257:1112–1126

Hanaoka S, Nagadoi A, Nishimura Y (2005) Comparison between TRF2 and TRF1 of their telomeric DNA-bound structures and DNA-binding activities. Protein Sci 14:119–130

Hess B, Bekker H, Beredensen H, Faraaije J (1997) LINCS: a linear constraint solver for molecular simulations. J Comput Chem 18:1463–1472

Hess B, Kutzner C, Spoel D, Lindahl E (2008) GROMACS 4: algorithms for highly efficient, load-balanced, and scalable molecular simulation. J Chem Theory Comput 4:435–447

Hu H, Zhang Y, Zou M, Yang S, Liang X (2010) Expression of TRF1, TRF2, TIN2, TERT, KU70, and BRCA1 proteins is associated with telomere shortening and may contribute to multistage carcinogenesis of gastric cancer. J Cancer Res Clin Oncol 136:1407–1414

Jason A, Stewart F, Chaiken W, Carolyn M (2012) Maintaining the end: roles of telomere proteins in end-protection, telomere replication and length regulation. Mut Res 730:12–19

Kim S, Kaminker P, Campisi J (1999) TIN2, a new regulator of telomere length in human cells. Nature Genet 23:405–412

Kim H, Lee O, Xin H, Chen L, Qin J, Chae H, Lin S, Safari A, Liu D, Songyang Z (2009) TRF2 functions as a protein hub and regulates telomere maintenance by recognizing specific peptide motifs. Nat Struct Mol Biol 16:372–379

Lei M, Podell E, Cech T (2004) Structure of human POT1 bound to telomeric single-stranded DNA provides a model for chromosome end-protection. Nat Struct Mol Biol 11:1223–1229

Liu D, O'Connor M, Qin J, Songyang Z (2004) Telosome, a mammalian telomere-associated complex formed by multiple telomeric proteins. J Biol Chem 279:51338–51342

Makov G, Payne M (1995) Periodic boundary conditions in ab initio calculations. Phys Rev B: Condens Matter 51:4014–4022

Okamoto K, Iwano T, Tachibana M, Shinkai Y (2008) Distinct Roles of TRF1 in the Regulation of telomere Structure and Lengthening. J Biol Chem 283:23981–23988

Sheu S, Yang D, Selzle H, Schlag E (2003) Energetics of hydrogen bonds in peptides. Proc Natl Acad Sci USA 100:12683–12687

Shrake A, Rupley J (1973) Environment and exposure to solvent of protein atoms. Lysozyme and insulin. J Mol Biol 79:351–371

Smogorzewska A, vanSteensel B, Bianchi A, Oelmann S, Schaefer M, Schnapp G, deLange T (2000) Control of human telomere length by TRF1 and TRF2. Mol Cell Biol 20:1659–1668

Takano K, Yamagata Y, Yutani K (2003) Buried water molecules contribute to the conformational stability of a protein. Protein Eng 16:5–9

vanGunsteren W, Mark A (1992) On the interpretation of biochemical data by molecular dynamics computer simulation. Eur J Biochem 204:947–961

vanSteensel B, Smogorzewska A, deLange T (1998) TRF2 protects human telomeres from end-to-end fusions. Cell 92:401–413

Walker J, Zhu X (2012) Post-translational modifications of TRF1 and TRF2 and their roles in telomere maintenance. Mech Ageing Dev 133:421–434

Weisi L, Zhang Y, Liu D, Songyanga Z, Wanb M (2013) Telomeres-structure, function, and regulation. Exp Cell Res 319:133–141

Xin H, Liu D, Wan M, Safari A, Kim H, Sun W, O'Connor M, Matthew S, Zhou S (2007) TPP1 is a homologue of ciliate TEBP-beta and interacts with POT1 to recruit telomerase. Nature 445:559–562

Ye J, Hockemeyer D, Krutchinsky A, Loayza D, Hooper S, Chait B, deLange T (2004a) POT1-interacting protein PIP1: a telomere length regulator that recruits POT1 to the TIN2/TRF1 complex. Genes Develop 18:1649–1654

Ye J, Donigian J, vanOverbeek M, Loayza D, Luo Y, Krutchinsky A, Chait B, deLange T (2004b) TIN2 Binds TRF1 and TRF2 Simultaneously and Stabilizes the TRF2 Complex on telomeres. J Biol Chem 279:47264–47271